CHAPTER 5

DISCUSSION AND FUTURE WORK

5.1 Discussion

The solution to sound scattering from concentric fluid spheres was first presented. The results were then verified by comparing to the single sphere solution of Anderson [8]. This solution is then later used to obtain data for use in verifying the wavefront reconstruction and ray tracing techniques. This solution is also currently being used to verify a finite element code developed by Dr. Margaret Wismer that will then be used to simulate sound scattering from the human head. Additional applications of this solution include approximating sound scattering from ultrasound contrast agents or cells. The Fourier pulse synthesis method was then derived as a means of performing simulations of finite duration pulses from the time-harmonic solution for scattering from concentric fluid spheres.

Multiple methods were presented to determine wavefronts from pressure data. The first method presented attempted to find the wavefront directly by finding the point that maximized the correlation with a time-shifted reference pulse. This method works well for weak scatterers but fails when the pulse amplitude varies. The remaining methods used an indirect approach to determine the wavefront. The arrival time of the pulse was first determined and then the wavefront was extracted as the set of points with the same arrival time. The first method of this kind used a simple cross correlation between the pulse at a point and a reference pulse. The arrival time was the shift of the reference signal that maximized the cross correlation. This method also works well for weak scatterers but fails when strong reflections occur. The next method used a frequency domain approach to determine arrival times. Since the delay information of a signal is contained in the phase information of a signal, by minimizing the phase, one can determine the arrival time of a

pulse. In theory this should work, but the problem of unwrapping the phase leads to unreliable results. The next method presented determined the arrival time by finding the first peak in the pulse. When noise is not present, this method works well and is fairly accurate. Noise introduces peaks before the onset of the pulse and therefore performs poorly when noise is present. The next method was based on the assumption that the waveform at the position behind the current one is nearly identical to the current one with some time shift. By determining this time shift, one can determine the arrival time between two points. By adding the arrival time differences over the domain, the arrival time can be determined. This method had two main drawbacks. First, the method had a tendency to underestimate the delay when strong reflections occurred. The method was also recursive in nature so the error tended to accumulate as the wavefront progressed. The final method proposed combined the last two methods to achieve the precision of the peak detection method while minimizing the error caused by noise. This was done by first using the peak detection method. If the result was within an acceptable range relative to the last arrival time, the peak detection result was used. If not, the difference in arrival times was computed using the cross correlation of the current signal with the last signal. This method was found to be accurate for most cases and was used for all ray tracing simulations performed later on.

A ray tracing technique for discretized domains was then presented. The idea behind the technique was to break the discretized wavefronts into a series of triangles. From these triangles it is straightforward to compute both the normal of the wavefront and the intersection of a ray with the wavefront. The topic of wavefront was revisited to address the issue of ray quantization. It was shown that the discretization of the wavefronts also discretized the ray directions achievable. This finite set of ray directions impacts the accuracy of the ray tracing computation, so a simple method of reducing the effect of this quantization was presented. The ray tracing technique was then verified by comparing simulation results with Snell's law. The verification showed good agreement with Snell's law. As the error began to increase it was shown that this error was not due to the method but due to the wavelength approaching the size of the sphere.

5.2 Future Work

The ultimate goal of this work is to apply the ray tracing code to FEM simulations of sound wave propagation into the human head. Before that can be done, the ray tracing code still needs to be verified for a wider range of scatterers. The technique was verified in this work for small changes in sound speed (300 m/s to 500 m/s) and no change in density. The human head has a much greater change in sound speed (343 m/s to 3000 m/s) and large changes in density (1 kg/m^3 to 2000 kg/m^3). Accordingly, the code should be verified for this range of values of density and sound speed. The first verification should compare the results of the code with Snell's law as was done here but for a range of sound speeds from 300 m/s to 3000 m/s for matched densities. The single sphere solution could then be used with changes in both sound speed and density in the ranges of interest.

After adequate verification of the ray tracing has been performed, it can then be applied to simulations of the human head. A preliminary model is currently being simulated. This particular model was made from CT scans of the dry human skull shown in Fig. 5.1. A layer of skin was then added by "growing" the skull and then subtracting the original skull. A rendering is shown in Fig. 5.2. The figure also shows a set of ear plugs which was added to the model to see if the occlusion effect is observed with the model. Finally, a brain was added by filling in the volume inside the skull as shown in Fig. 5.3. As can be seen from the renderings, the model is not an accurate representation of a human head. The skin is attached directly to the skull and is missing much of a tissue that would make the model have a more human-like face. The model is also missing the outer ears and nose. A second model is currently being developed using data from a human cadaver. This should be a better representation of a human head since the outer ears, skin, and nose are still intact.

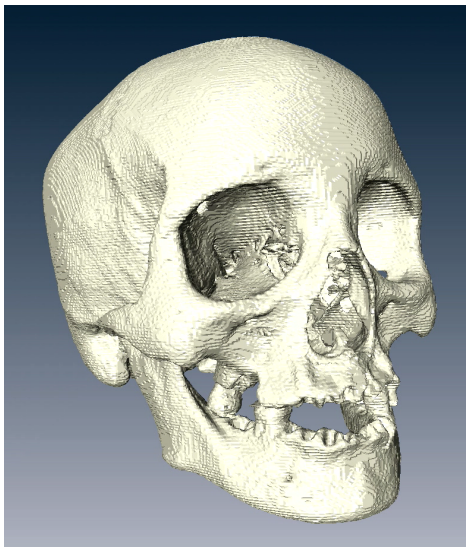

Figure 5.1: Rendering of skull used for finite element simulation.

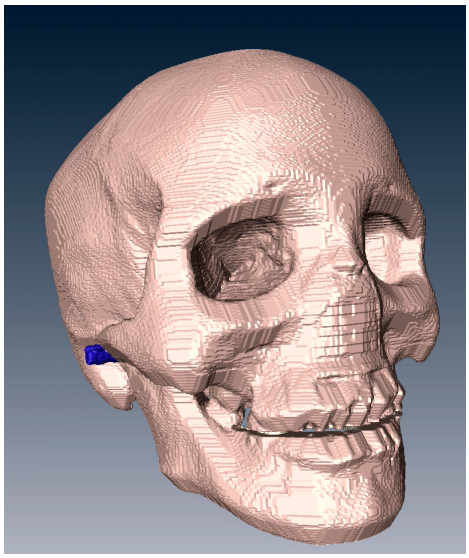

Figure 5.2: Rendering of skull used for finite element simulation with skin layer added.

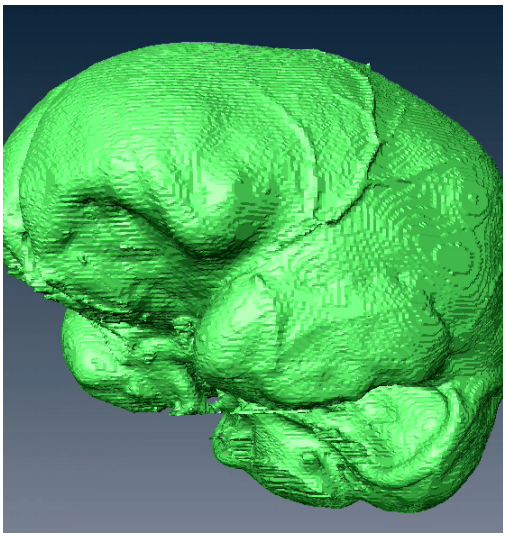

Figure 5.3: Rendering of brain added to model used for finite element simulation.